

## DIELECTRIC BREAKDOWN ELIMINATION VIA PARTICULATE ADDITIVES

T. I. Zohdi

*Department of Mechanical Engineering*

*6195 Etcheverry Hall*

*University of California, Berkeley, CA, 94720-1740, USA*

*email: zohdi@newton.berkeley.edu*

**Abstract.** In many materials, strong electrical fields can cause highly conductive pathways to occur due to *dielectric breakdown*, which can cause the material to “jump” to a higher permittivity state. This effect is often undesirable and can lead to electrically-induced failure of a device, for example due to overheating. The overall goal of this work is to estimate the volume fraction and properties of the particulate additives needed to reduce the electrical load carried by a bulk material, in order to avoid dielectric breakdown.

**Keywords:** effective permittivity, dielectric breakdown

**1 Introduction.** Many electronic devices experience fluctuating electrical loads levels during the course of their operation. Frequently, a material with a low dielectric constant is selected where, at sufficiently high electrical field strengths, the dielectric constant jumps to a higher value, due to dielectric breakdown. This occurs when an applied field is strong enough to mobilize free electrons that are present in a medium so that they attain sufficiently large energies to dislodge other electrons, resulting in a large number of free electrons and positively charged ions. The dislodged electrons then repeat the procedure in a chain-like reaction manner, which results in a higher permittivity. This effect can lead to electronic device failure. However, in many cases, the material that has been selected for the application at hand has other desirable qualities, such as being inexpensive, easy to form, a favorable thermal conductivity, etc. Thus, the material designer must seek ways by which to modify the chosen material, for example by employing particulate additives, so that they can retain the use of the original material, but avoid dielectric breakdown. Therefore, the central question is: *What should be the proper particulate properties, such as volume fraction and permittivity, in order to keep the electrical field strength in the surrounding (bulk matrix) material below a critical threshold value?*

In the context of electrical materials (Figure 1), the microscale properties are characterized by a spatially variable permittivity  $\epsilon(\mathbf{x})$ . Typically, in order to characterize the structural-scale effective response of such materials, a relation between averages

$$\langle \mathbf{D} \rangle_{\Omega} = \epsilon^* \cdot \langle \mathbf{E} \rangle_{\Omega}, \quad (1)$$

is sought, where  $\langle \cdot \rangle_{\Omega} \stackrel{\text{def}}{=} \frac{1}{|\Omega|} \int_{\Omega} \cdot d\Omega$  is the volume averaging operator,  $\mathbf{D}$  is the electrical flux (density) and  $\mathbf{E}$  is the electric field within a statistically representative volume element (RVE) of volume  $|\Omega|$ . The quantity,  $\epsilon^*$ , is known as the effective permittivity, and is the property used in usual (homogenized) macroscale analyses.

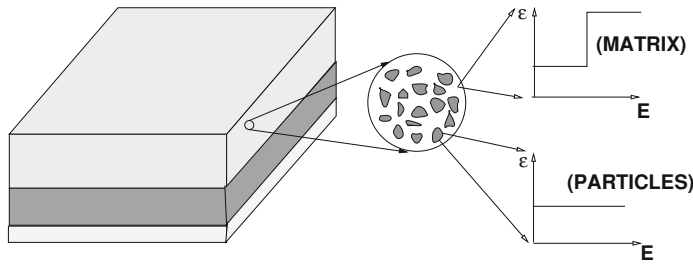


Figure 1: A material with particulate additives.

We consider a two-phase particulate-matrix material combination. Specifically, the case of interest here is one where we seek particulate additives to take the electrical load off of the surrounding bulk matrix material, below a threshold value:  $\|\langle \mathbf{E} \rangle_{\Omega_1}\| \leq E_{crit}$ , where  $E_{crit}$  corresponds to the critical value of the magnitude of the field to permit dielectric breakdown and  $\Omega_1$  is the matrix (bulk material) domain. In order to determine the properties of the particulates, volume fractions, etc, needed to obey this restriction, we need to develop estimates of the electric field carried by the particulates and the matrix material.

**2 Phase-wise electrical load-levels.** One can determine the electrical “load level” carried by each phase by considering the following identities:

$$\langle \mathbf{E} \rangle_{\Omega} = \frac{1}{|\Omega|} \left( \int_{\Omega_1} \mathbf{E} \, d\Omega + \int_{\Omega_2} \mathbf{E} \, d\Omega \right) = v_1 \langle \mathbf{E} \rangle_{\Omega_1} + v_2 \langle \mathbf{E} \rangle_{\Omega_2} \quad (2)$$

$$\langle \mathbf{D} \rangle_{\Omega} = \frac{1}{|\Omega|} \left( \int_{\Omega_1} \mathbf{D} \, d\Omega + \int_{\Omega_2} \mathbf{D} \, d\Omega \right) = v_1 \langle \mathbf{D} \rangle_{\Omega_1} + v_2 \langle \mathbf{D} \rangle_{\Omega_2}, \quad (3)$$

where  $v_1$  and  $v_2$  are the volume fractions of phases 1 and 2 respectively, so that  $v_1 + v_2 = 1$ . Performing straightforward algebraic manipulations yields

$$\begin{aligned} \langle \mathbf{D} \rangle_{\Omega} &= v_1 \langle \mathbf{D} \rangle_{\Omega_1} + v_2 \langle \mathbf{D} \rangle_{\Omega_2} \\ &= v_1 \epsilon_1 \cdot \langle \mathbf{E} \rangle_{\Omega_1} + v_2 \epsilon_2 \cdot \langle \mathbf{E} \rangle_{\Omega_2} \\ &= \epsilon_1 \cdot (\langle \mathbf{E} \rangle_{\Omega} - v_2 \langle \mathbf{E} \rangle_{\Omega_2}) + v_2 \epsilon_2 \cdot \langle \mathbf{E} \rangle_{\Omega_2} \\ &= \underbrace{(\epsilon_1 + v_2(\epsilon_2 - \epsilon_1) \cdot \mathbf{C}_{E,2})}_{\epsilon^*} \cdot \langle \mathbf{E} \rangle_{\Omega}, \end{aligned} \quad (4)$$

where

$$\underbrace{\left( \frac{1}{v_2} (\epsilon_2 - \epsilon_1)^{-1} \cdot (\epsilon^* - \epsilon_1) \right)}_{\stackrel{\text{def}}{=} \mathbf{C}_{E,2}} \cdot \langle \mathbf{E} \rangle_{\Omega} = \langle \mathbf{E} \rangle_{\Omega_2}. \quad (5)$$

$\mathbf{C}_{E,2}$  is known as the electric field concentration tensor. In the special case of isotropy,  $\mathbf{C}_{E,2} = C_{E,2}\mathbf{1}$ , where

$$C_{E,2} = \frac{1}{v_2} \frac{\epsilon^* - \epsilon_1}{\epsilon_2 - \epsilon_1}. \quad (6)$$

Once either  $\mathbf{C}_{E,2}$  or  $\epsilon^*$  are known, the other can be determined. We have from Equation 2

$$\langle \mathbf{E} \rangle_{\Omega_1} = \frac{\langle \mathbf{E} \rangle_{\Omega} - v_2 \langle \mathbf{E} \rangle_{\Omega_2}}{v_1} = \frac{(\mathbf{1} - v_2 \mathbf{C}_{E,2}) \cdot \langle \mathbf{E} \rangle_{\Omega}}{v_1} \stackrel{\text{def}}{=} \mathbf{C}_{E,1} \cdot \langle \mathbf{E} \rangle_{\Omega}, \quad (7)$$

where

$$\mathbf{C}_{E,1} = \frac{1}{v_1} (\mathbf{1} - v_2 \mathbf{C}_{E,2}) = \frac{\mathbf{1} - v_2 \mathbf{C}_{E,2}}{1 - v_2} \quad (8)$$

and in the case of isotropy

$$C_{E,1} = \frac{1 - v_2 C_{E,2}}{1 - v_2} = \frac{1}{1 - v_2} \frac{\epsilon_2 - \epsilon^*}{\epsilon_2 - \epsilon_1}. \quad (9)$$

The concentration tensors indicate the amplification or reduction of the field within the phases relative to the overall field average.

**3 Individual and overall dielectric breakdown.** Since the field in the matrix material can be written as  $\mathbf{C}_{E,1} \cdot \langle \mathbf{E} \rangle_{\Omega}$  and must be restricted by  $\|\langle \mathbf{E} \rangle_{\Omega_1}\| \leq E_{crit}$ , to avoid dielectric breakdown, one may solve for a corresponding volume fraction to avoid the breakdown in the matrix phase (assuming material isotropy)

$$\|\langle \mathbf{E} \rangle_{\Omega_1}\| = \|\mathbf{C}_{E,1} \cdot \langle \mathbf{E} \rangle_{\Omega}\| \leq E_{crit} \Rightarrow v_2 \leq v_2^* \stackrel{\text{def}}{=} 1 - \frac{\epsilon_2 - \epsilon^*}{\epsilon_2 - \epsilon_1} \frac{\|\langle \mathbf{E} \rangle_{\Omega}\|}{E_{crit}}, \quad (10)$$

where  $v_2^*$  is a restriction that must be obeyed so that the critical field can be avoided in phase 1. However, because  $\epsilon^* = \mathcal{F}(\epsilon_1, \epsilon_2, v_2)$ , there is no guarantee that the material combination  $\epsilon_1, \epsilon_2, v_2$  may satisfy this inequality. To determine whether this combination of parameters is feasible, we employ bounding principles.

**4 Effective property bounds.** Direct computation of the effective properties is complex, since it requires a very fine spatial discretization to resolve the microstructural features of the material in order to determine the electric field throughout the material. Accordingly, a variety of approximation techniques have been developed to estimate the overall macroscopic properties of materials consisting of a matrix, containing a uniform distribution of particles, in terms of the individual phase volume fractions and properties. For example, consider the widely used the Hashin-Shtrikman bounds (Hashin and Shtrikman (1962)) for isotropic materials (such as an isotropic matrix with randomly dispersed isotropic particles)

$$\underbrace{\epsilon_1 + \frac{v_2}{\frac{1}{\epsilon_2 - \epsilon_1} + \frac{1-v_2}{3\epsilon_1}}}_{\epsilon^{*, -}} \leq \epsilon^* \leq \underbrace{\epsilon_2 + \frac{1-v_2}{\frac{1}{\epsilon_1 - \epsilon_2} + \frac{v_2}{3\epsilon_2}}}_{\epsilon^{*, +}}, \quad (11)$$

where  $\epsilon_2 \geq \epsilon_1$ ,  $v_2$  is the volume fraction of phase with the higher  $\epsilon$  value (“phase 2” in the former expression) for the permittivity-mismatch. Such bounds are the tightest for isotropic effective responses, with isotropic two phase microstructures, where only the volume fractions and phase contrasts of the constituents are known. Note that no further geometric information, such as the number and nature of particles, etc., contributes to these bounds. The usual assumptions that the particulate material microstructure satisfies ergodicity requirements are assumed to hold. For more on ergodic hypotheses see the classical work of Kröner (1972).

**Remarks:** The lower bound is typically more accurate for microstructures where high permittivity particles are surrounded by a low permittivity matrix, while the upper bound is more accurate for a high permittivity matrix surrounding low permittivity particles. This can be explained qualitatively in the following manner. Consider a heterogeneous material with 50 % low permittivity material and 50 % high permittivity material. Now consider a case (Case 1) where the matrix material is made of the high permittivity material and the particles are comprised of the low permittivity material. In the opposite case (Case 2), the matrix material is made of the low permittivity material and the particles are comprised of the high permittivity material. The bounds in this case are the same, however, the overall permittivity in Case 1 is higher than the overall permittivity in Case 2. Clearly, Case 1 is more closely approximated by the upper bound and Case 2 is closer to the lower bound. We remark that there is a direct analogy to the elastic properties of a material comprised of a stiff (high permittivity) matrix with embedded soft (low permittivity) inclusions versus a material comprised of a soft (low permittivity) matrix containing hard (high permittivity) inclusions.

**5 Feasibility via inversion of the bounds.** After straightforward manipulations, the Hashin-Shtrikman bounds may be inverted to solve for “feasibility” bounds on  $v_2^*$

$$\underbrace{\frac{(\epsilon^* - \epsilon_1)3\epsilon_2}{(\epsilon^* + 2\epsilon_2)(\epsilon_1 - \epsilon_2)}}_{\stackrel{\text{def}}{=} v_2^-} \leq v_2^* \leq \underbrace{\frac{(\epsilon^* - \epsilon_1)(2\epsilon_1 + \epsilon_2)}{(2\epsilon_1 + \epsilon^*)(\epsilon_2 - \epsilon_1)}}_{\stackrel{\text{def}}{=} v_2^+}, \quad (12)$$

where inverting the upper bound Hashin-Shtrikman bound generates  $v_2^-$  and inverting the lower bound Hashin-Shtrikman bound generates  $v_2^+$ .

Figure 2 illustrates an example where  $\epsilon_2/\epsilon_0 = 20$  and  $\epsilon_1/\epsilon_0 = 1$ . The value of  $\epsilon^*/\epsilon_0$  is computed, for the range where the bounds are satisfied.<sup>1</sup> Outside of the plotted ranges, the feasibility bounds are violated. The estimates can be made tighter

<sup>1</sup> $\epsilon_0$  is the vacuum permittivity.

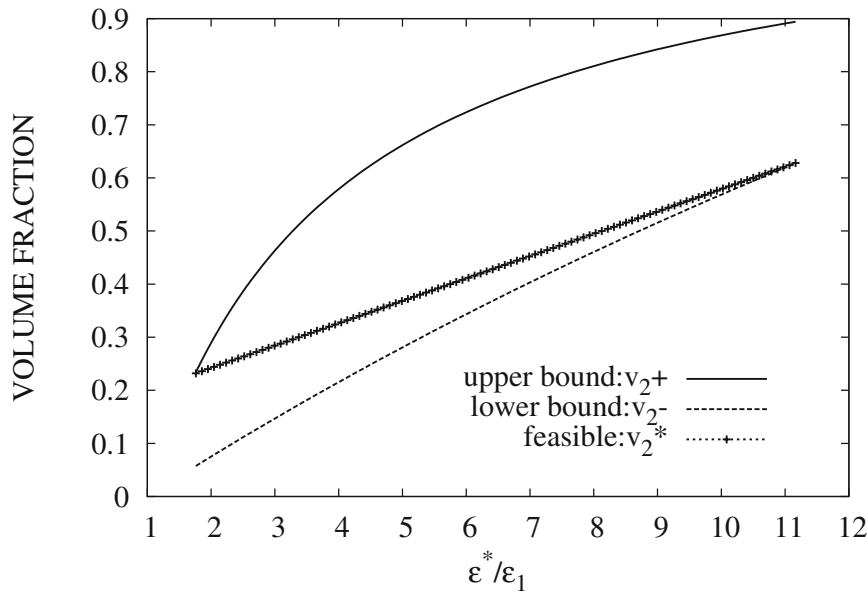


Figure 2: Depicted above are the curves for the upper ( $v_2^+$ ) and lower ( $v_2^-$ ) bounds and the feasible volume fractions ( $v_2^*$ ) for  $\epsilon_2/\epsilon_1 = 20$ . At the left end of the feasible range of parameters, the upper bound is attained ( $v_2^* = v_2^+$ ), and at the right end of the feasible range, the lower bound is attained ( $v_2^* = v_2^-$ ).

by realizing that the feasible estimate,  $v_2^*$ , is in fact an upper bound, thus the true volume fraction ( $v_2$ ) obeys

$$v_2^- \text{ (lower bound)} \leq v_2 \leq v_2^* \text{ (feasible)}. \tag{13}$$

**Remark 1:** Equation 10 may be recast in terms of the electric field

$$\frac{\|\langle \mathbf{E} \rangle_\Omega\|}{E_{crit}} \leq \frac{\epsilon_2 - \epsilon_1}{\epsilon_2 - \epsilon^*} (1 - v_2) \tag{14}$$

and the feasibility bounds as

$$(1 - \Theta) \frac{\epsilon_2 - \epsilon_1}{\epsilon_2 - \epsilon^*} \leq \frac{\|\langle \mathbf{E} \rangle_\Omega\|}{E_{crit}} \leq (1 - \Phi) \frac{\epsilon_2 - \epsilon_1}{\epsilon_2 - \epsilon^*}, \tag{15}$$

where

$$\Theta \stackrel{\text{def}}{=} \frac{(3\epsilon_1 + (\epsilon_1 - \epsilon_2))(\epsilon^* - \epsilon_1)}{(3\epsilon_1 + (\epsilon^* - \epsilon_2))(\epsilon_2 - \epsilon_1)} \quad \text{and} \quad \Phi \stackrel{\text{def}}{=} \frac{3\epsilon_2(\epsilon_1 - \epsilon^*)}{(\epsilon^* + 2\epsilon_2)(\epsilon_1 - \epsilon_2)}. \tag{16}$$

These estimates provide the limits on the applied electric field to avoid dielectric breakdown.

**Remark 2:** The procedure for determining the feasible volume fractions is virtually the same for electrical and mechanical fields where, instead of Equation 1, one has (linear elasticity)

$$\langle \boldsymbol{\sigma} \rangle_{\Omega} = \mathbf{IE}^* : \langle \boldsymbol{\varepsilon} \rangle_{\Omega}, \quad (17)$$

where  $\boldsymbol{\sigma}$  and  $\boldsymbol{\varepsilon}$  are the stress and strain fields, and  $\mathbf{IE}^*$  is the effective stiffness tensor. In this case, the analogous field restrictions would be on the average strain carried by the matrix phase.

**Remark 3:** In the case of anisotropy, Equations 5 and 8 yield

$$v_2 \leq v_2^* \stackrel{\text{def}}{=} 1 - \frac{1}{E_{crit}} \left\| \left( \mathbf{1} - (\boldsymbol{\varepsilon}_2 - \boldsymbol{\varepsilon}_1)^{-1} \cdot (\boldsymbol{\varepsilon}^* - \boldsymbol{\varepsilon}_1) \right) \cdot \langle \mathbf{E} \rangle_{\Omega} \right\|. \quad (18)$$

However, in the case of anisotropy, the bounds in Equation 11 are inapplicable. For information on anisotropic effective property bounds, see Hashin (1983). In some cases, bounds may not be possible, however accurate estimates on the effective properties can still be achieved. For example, see Sevostianov et al (2001).

**6 Discussion.** *In principle, the approach introduced here can be used with other bounding or estimation techniques.* Provided that the desired state is feasible, the actual microstructure that may achieve it would need to be generated numerically by solving a boundary-value problem posed over an RVE domain. Such numerical simulations are time-consuming, especially if they involve numerous trial runs during an optimization procedure. In general, to streamline computations, one can determine an initial estimate on the volume fraction needed to deliver a certain desired effective property by using the developed analytical results, and then refine the choice of particulate properties, phase morphology, etc, using numerical methods. Direct numerical techniques for heterogeneous electromagnetic and elastic media can be found in, for example, Zohdi (2003, 2008).

The identification of microstructural parameters which force the system behavior to match a (desired) effective response will usually lead to a nonconvex inverse problem (multiple feasible solutions). For example, consider inverse problems whereby microstructural quantities such as (1) the properties of the particles (2) the volume fraction of the particles and (3) the topological parameters of the particles are sought which deliver a desired overall response by minimizing the difference between the desired overall permittivity ( $\boldsymbol{\varepsilon}^{*,D}$ ) and the predicted value ( $\boldsymbol{\varepsilon}^*$ ), along with constraints,

$$\Pi = \left( \frac{\|\boldsymbol{\varepsilon}^* - \boldsymbol{\varepsilon}^{*,D}\|}{\|\boldsymbol{\varepsilon}^{*,D}\|} \right)^2 + \text{constraints}. \quad (19)$$

Generally,  $\Pi$  will depend on the design variables in a nonconvex manner on the microstructural parameters. Nonconvexity can lead to problems for standard gradient-based minimization techniques which, however, can be mitigated by employing a global-local search procedure based on initially using “gradient-less” types of minimization, such as “genetic” algorithms (global search), before applying classical (local convex search) gradient-based schemes. Genetic algorithms are search methods based on the principles of natural selection, drawing upon concepts of species evolution, such as reproduction, mutation and crossover. Implementation typically

involves a randomly generated population of “genetic” strings, each of which represents a specific choice of system parameters. The population of genes undergo “mating sequences”, “offspring production” and other biologically-inspired events in order to find regions of the search space where cost functions are small. These methods date back, at least, to pioneering work Holland (1975). For general reviews, see Goldberg and Deb (2000). We refer the reader to Zohdi (2003) for specific genetic algorithms to treat inverse problems involving various particulate systems.

## References

1. Goldberg, D. E. and Deb, K. 2000. Special issue on Genetic Algorithms. *Computer Methods in Applied Mechanics and Engineering*. 186 (2-4) 121-124.
2. Hashin, Z. and Shtrikman, S. 1962. A variational approach to the theory of effective magnetic permeability of multiphase materials. *Journal of applied Physics*, volume 33, no. 10, pp 3125-3131.
3. Hashin, Z. 1983. Analysis of composite materials: a survey. *ASME Journal of Applied Mechanics*. **50**, 481-505.
4. Holland, J. H. 1975. *Adaptation in natural and artificial systems*. Ann Arbor, Mich. University of Michigan Press.
5. Kröner, E. 1972. *Statistical Continuum Mechanics*. CISM Lecture Notes. **92**, Springer-Verlag.
6. Sevostianov, I., Gorbatiikh, L. and Kachanov, M. 2001. Recovery of information of porous / microcracked materials from the effective elastic / conductive properties. *Materials Science and Engineering. A* 318, 1-14.
7. Zohdi, T. I. 2003. Genetic optimization of statistically uncertain microheterogeneous solids. *Philosophical Transactions of the Royal Society: Mathematical, Physical & Engineering Sciences*. Vol: 361, No: 1806, 1021 – 1043
8. Zohdi, T. I. 2008. On the computation of the coupled thermo-electromagnetic response of continua with particulate microstructure. *The International Journal of Numerical Methods in Engineering*. **76**, 1250-1279.